Research Article

Mohammed Azmi Al-Betar*, Zaid Abdi Alkareem Alyasseri, and Sharif Naser Makhadmeh

EEG channels selection for stroke patients rehabilitation using equilibrium optimizer

https://doi.org/10.1515/jisys-2024-0252
received May 07, 2024; accepted July 15, 2024

Abstract: Stroke ranks as the second leading cause of death worldwide and is a major contributor to disability. Researchers have proposed various applications to assist in the rehabilitation of stroke patients, with brain-computer interfaces (BCIs) utilizing electroencephalograms (EEGs) showing particularly promising outcomes. However, the most challenging aspect of using BCI methods is effectively extracting and selecting the most significant features from the vast amount of EEG data available. This article addresses this problem by presenting an innovative optimization-based approach to the channel selection problem, employing a novel binary equilibrium optimizer (EO) as an optimization technique to identify the most relevant EEG channels. This method significantly enhances the accuracy of stroke patient rehabilitation outcomes while reducing computational complexity, avoiding overfitting, and minimizing user discomfort during clinical use. During the preprocessing step, conventional filters and the AICA-WT (automatic independent component analysis with wavelet transform) denoising technique are employed. Attributes are then computed for the time, entropy, and frequency domains. The EO algorithm is utilized to represent the EEG channel selection problem, transforming the features of each individual EEG into binary values and subsequently applying a k-nearest neighbor classifier technique to determine the accuracy rate. The proposed method demonstrates superior performance, achieving the highest accuracy rate of 99% with the HFD features, compared to the existing methods. In general, the proposed study provides a more reliable strategy by identifying a subject-specific reduced set of relevant electrodes and establishes a new benchmark in the field of stroke rehabilitation, highlighting the quality and potential impact of this work.

Keywords: EEG, feature extraction, stroke patients, metahurstic algorithms, equilibrium optimizer

1 Introduction

The World Health Organization (WHO) considers stroke as the second leading cause of death globally due to its detrimental effects on the brain resulting from disruptions in cerebral circulation [1,2]. Hemiplegia, a severe form of motor impairment characterized by partial or complete paralysis of one side of the body, including the arm, leg, foot, and hand, is one of the most debilitating consequences of stroke. Ischemic stroke, the most common type, leads to a sudden loss of brain function due to interrupted cerebral perfusion [3,4]. More than 60% of stroke survivors require rehabilitation to address permanent motor function impairments [5]. However, stroke survivors often experience a range of disabilities, including visual and cognitive deficits, which

* **Corresponding author: Mohammed Azmi Al-Betar**, Artificial Intelligence Research Center (AIRC), College of Engineering and Information Technology, Ajman University, Ajman, P.O. Box: 346, United Arab Emirates; Hourani Center for Applied Scientific Research, Al-Ahliyya Amman University, 19328, Amman, Jordan, e-mail: m.albetar@ajman.ac.ae
Zaid Abdi Alkareem Alyasseri: Information Technology Research and Development Center (ITRDC), University of Kufa, Najaf, 54001, Iraq; College of Engineering, University of Warith Al-Anbiyaa, 56001, Karbala, Iraq, e-mail: zaid.alyasseri@uokufa.edu.iq
Sharif Naser Makhadmeh: Department of Information Technology, King Abdullah II School for Information Technology, University of Jordan (UJ), 11942 Amman, Jordan, e-mail: s_makhadmeh@ju.edu.jo

severely impact their ability to perform even basic tasks. Consequently, extensive research has been conducted to develop effective treatments and rehabilitation strategies for stroke patients [6].

Electroencephalography (EEG) is a noninvasive method used to measure the electrical activity of the brain with high temporal resolution, providing insights into various mental tasks [7,8]. Brain–computer interfaces (BCIs) enable individuals with physical impairments to interact with the external world by translating brain EEG signals into control commands [9,10]. Motor imagery (MI) is a technique where individuals mentally simulate body movements without actual muscle activation, and the associated rhythmic brain activities can be recorded and utilized as input signals for BCI systems. Event-related desynchronization/synchronization (ERD/ERS) refers to the changes in rhythmic power within specific frequency bands, such as mu (8–12 Hz) and beta (13–30 Hz), in the sensorimotor area during MI tasks. These changes can be leveraged to distinguish between different types of MI tasks [7]. BCIs based on MI have gained popularity due to their ability to operate without the need for external stimuli [11]. However, the complex and volatile nature of EEG signals poses challenges in decoding MI-based BCIs using conventional methods [9]. Effective feature extraction and reliable classification of various MI tasks from low signal-to-noise EEG data remain critical and difficult tasks [7].

Preprocessing raw EEG signals is crucial for accurate classification in MI-based signal analysis since recorded wave activities can be corrupted by various artifacts. Artifacts such as eye blinks, ocular movements, cardiac activity, muscular interference, and power line noise can distort EEG signals, affecting their frequencies [12]. Evaluating the efficiency of EEG signals in the presence of background noise can be challenging. Spatial filters can improve the localization of signals for each electrode as EEG-based BCIs typically have poor spatial resolution [11].

Feature extraction is performed on recorded EEG channels in multiple domains to identify the best features for BCI MI-based analysis. Common spatial pattern (CSP) is a popular technique for obtaining discriminative features from high-dimensional EEG signals and has been used to identify spatial characteristics related to ERD during various MI tasks [13]. However, the effectiveness of CSP is influenced by noise and the selection of frequency bands. To address this issue, various feature extraction techniques have been developed to analyze EEG data in the time, frequency, and time–frequency domains [14,15].

The classifier's performance significantly deteriorates with an increasing number of features due to the curse of dimensionality, which occurs when the feature count exceeds a certain threshold. This phenomenon leads to overfitting, where the model captures noise rather than the underlying patterns, thereby reducing generalization capability. Moreover, higher feature dimensionality leads to longer training procedures, escalating computational costs and resource demands, which are impractical in clinical settings where timely decision-making is crucial [16]. Thus, addressing the curse of dimensionality is paramount to enhance the classifier's performance and ensure the feasibility of BCI applications in real-world stroke rehabilitation scenarios.

To identify a large number of existing channels, feature selection is necessary, involving a comprehensive search for relevant channels that provide the most valuable data while minimizing redundancy [17–19]. Previous studies have focused on feature selection and proposed methods such as complete search, greedy search, and random search [20]. However, these selection techniques suffer from high computational costs, making them inefficient and often infeasible for practical applications. In addition, these methods are prone to the issue of converging to local optima, which limits their ability to identify the most relevant features effectively. This highlights the critical need for more efficient and robust optimization techniques to improve feature selection, reduce computational overhead, and enhance the overall performance and reliability of BCI systems in stroke rehabilitation.

This research focuses on the selection of channels. Numerous electrodes are used in medical and diagnostic procedures. For practical BCI applications, the accuracy of classification achieved using multiple electrodes is crucial. However, the process of applying electrodes to the scalp is time-consuming and challenging, and using numerous electrodes for EEG extraction leads to overfitting. Thus, it is essential to identify the electrodes that contribute minimally or not at all to categorization. Electrode selection can also assess neurological knowledge since individuals may react differently, and there may be changes in the optimal electrode positions specific to each subject. Automatic determination of electrode relevance is necessary for user-

dependent categorization tasks. This can be achieved by considering a wide range of electrodes initially and employing various approaches to select the best channels for each patient.

The main contributions of this study are summarized as follows:

(1) Particle equilibrium optimizer (EO) algorithm-based optimization technique is investigated and utilized to select the most relevant EEG channels for stroke patient rehabilitation. Each EEG channel provides a distinct set of features for classification. Channel selection reduces data storage and processing requirements by eliminating unnecessary dimensions, speeds up classifier training by using simpler data, and mitigates the curse of dimensionality to prevent overfitting.
(2) Raw EEG data are segmented and filtered using standard filters, and the automated independent component analysis with wavelet transform (AICA-WT) denoising approach is utilized to address the aforementioned issues.
(3) Time–entropy–frequency (TEF) attributes are created by combining effective features from the time, entropy, and frequency domains. The EO-based optimization method is employed to optimize the TEF characteristics and select efficient channels that enhance system stationarity and resilience.

A series of experiments are conducted to evaluate the proposed framework using 25 MI-based BCI sessions from public datasets of BCI Competition. Follow-up assessment visits were conducted to examine functional changes before and after EEG neurorehabilitation. The AICA-WT-TEF-Chs framework utilizing hybrid TEF attributes aims to effectively leverage the information from the time, entropy, and frequency domains for MI-BCI classification.

The rest of this article is organized as follows. Section 2 deeply describes the Eo algorithm and the proposed method utilized in this study. The main parameters and measurements used in this study are illustrated in Section 4. In addition, the section presented the obtained results by the proposed method and all comparisons with other competitive studies. Section 5 concludes this article.

2 EO

The EO is a metaheuristic algorithm introduced by [21]. It draws inspiration from control volume mass balance models, which are used to assess both dynamic and equilibrium conditions. In EO algorithm, each particle (solution) serves as a search agent, with its concentration (position) guiding the search. By iteratively updating their concentrations based on the best-so-far solutions, called equilibrium candidates, the search agents eventually converge to the equilibrium state, resulting in the optimal outcome.

2.1 Inspiration of EO

The EO draws its inspiration from the concept of mass balance applied to a control volume. This approach involves using the equation of mass balance to account for the concentration of nonreactive constituents within the control volume. The mass balance equation ensures that the inflow, outflow, and generation of mass within the control volume are taken into consideration and maintained. Several parameters need to be taken into account when formulating the mass balance equation, including the rate of change of mass over time, the amount of mass entering the control volume, the amount of mass generated within the control volume, and the amount of mass leaving the control volume. The formulation of the mass balance equation is as follows:

$$V\frac{\mathrm{d}C}{\mathrm{d}t} = QC_{\mathrm{eq}} - QC + G, \tag{1}$$

where V is the control volume, C presents the concentration amount in V, Q is the volumetric flow rate in and out of V, G is the mass generation rate in V, and C_{eq} denotes the equilibrium state concentration.

To obtain the concentration in the control volume, equation (1) can be rearranged in the following manner:

$$\mathrm{d}t = \frac{\mathrm{d}C}{\lambda C_{\text{eq}} - \lambda C + \frac{G}{V}} \tag{2}$$

subject to:

$$\lambda = \frac{Q}{V}.$$

By incorporating integration, equation (2) can be expressed as follows:

$$\int_{t_0}^{t} \mathrm{d}t = \int_{C_0}^{C} \mathrm{d}t \frac{\mathrm{d}C}{\lambda C_{\text{eq}} - \lambda C + \frac{G}{V}}. \tag{3}$$

This results in:

$$C = C_{\text{eq}} + (C_0 - C_{\text{eq}})F + \frac{G}{\lambda V}(1 - F). \tag{4}$$

Subject to:

$$F = \exp[-\lambda(t - t_0)].$$

The concentration in control volume V, given a known turnover rate, can be estimated using equation (4), where C_0 represents the initial concentration at time t_0. Furthermore, equation (4) can also be utilized to calculate the average turnover rate when the generation rate is known.

The aforementioned equations play a crucial role in controlling the search behavior of the EO. In the EO population, each particle corresponds to a solution, and the concentrations represent their positions (analogous to swarm algorithms). As described earlier in equation (4), the update mechanism for a particle's position and concentration involves three distinct terms: the equilibrium concentration, the concentration difference between the particle and the equilibrium state, and the generation rate. These terms collectively govern the adjustment of the particle's position and concentration during the optimization process.

2.2 Procedure of EO

The EO is a metaheuristic algorithm used for solving optimization problems. Here's a summary of the procedure based on the article you provided:

2.2.1 Initialization and function evaluation

Similar to other metaheuristics, the EO commences its optimization process by initializing various parameters. These include defining the minimum and maximum values for the dimensions (C_{min} and C_{max}, respectively) and specifying the number of particles (n) in the population. Furthermore, the EO initializes its initial population randomly. In this regard, the concentrations are initialized based on the number of particles and their dimensions, employing a random assignment within the search space. This initialization is carried out using the following formula:

$$C_i^{\text{initial}} = C_{\text{min}} + r_i \times (C_{\text{max}} - C_{\text{min}}). \tag{5}$$

subject to:

$$i = 1, 2, \ldots, n,$$

where C_i^{initial} is the initial concentration vector of particle i, and r_i represents a random vector within a range between 0 and 1.

2.3 Fitness function evaluation

During this step, all particles within the population undergo evaluation using the fitness function specific to the optimization problem at hand. Subsequently, the particles are sorted based on their corresponding fitness values. This sorting process allows for the identification of the equilibrium candidates among the particles, as those with better fitness values are considered more favorable solutions.

2.4 Equilibrium pool and candidates

Once the EO search process begins, equilibrium candidates are identified to establish the search pattern for the particles. Through extensive testing across different problem types, it has been determined that the best four equilibrium candidates exhibit superior performance during the optimization process. In addition, a fifth candidate is introduced, which represents the arithmetic mean of the four best candidates. This inclusion aims to strike a balance between exploration and exploitation capabilities within the EO. These five candidates are utilized to construct the equilibrium pool vector, as depicted below:

$$\vec{C}_{\text{eq,pool}} = \{\vec{C}_{\text{eq(1)}}, \vec{C}_{\text{eq(2)}}, \vec{C}_{\text{eq(3)}}, \vec{C}_{\text{eq(4)}}, \vec{C}_{\text{eq(ave)}}\}. \tag{6}$$

During each iteration of the EO, all particles update their concentrations by randomly selecting candidates with equal probabilities. For instance, in one iteration, a particle may update its concentrations based on $\vec{C}_{\text{eq(ave)}}$, while in the next iteration, the concentrations could be updated using $\vec{C}_{\text{eq(1)}}$. This process continues, with particles updating their concentrations using different candidates in a randomized manner, until the stop criterion is met. The stop criterion signifies the end of the optimization process.

2.5 Exponential term (F)

The exponential term (F) is employed to update the concentrations in the EO. F plays a crucial role in enhancing and achieving an optimal balance between exploration and exploitation during the search process. The calculation of F can be performed using the following formula:

$$\vec{F} = \exp^{-\vec{\lambda}(t-t_0)}, \tag{7}$$

where $\vec{\lambda}$ is a random vector within a range between 0 and 1 and t represents an iteration function that can be computed as follows:

$$t = \left(1 - \frac{\text{Iter}}{\text{Iter}_{\text{Max}}}\right)^{\left(a_2 \times \frac{\text{Iter}}{\text{Iter}_{\text{Max}}}\right)}, \tag{8}$$

where Iter and Iter_{Max} denote the current and the maximum number of iterations, respectively, and a_2 represents a static value. Equation (9) is utilized in the EO to enhance its convergence while simultaneously maintaining a balance between exploration and exploitation.

$$\vec{t_0} = \frac{1}{\lambda} \times \ln(-a_1 \text{sign}(\vec{r} - 0.5)[1 - \exp^{-\vec{\lambda} t}]) + t, \tag{9}$$

where a_1 is a static value. When a_1 is set to a higher value, it increases the exploration capability of the EO, resulting in a lower exploitation capability. Conversely, when a_2 is set to a higher value, it enhances the exploitation capability while reducing the exploration capability. The term $\text{sign}(\vec{r} - 0.5)$ is employed to influence the directions of exploration and exploitation. Here, $\vec{r}$ represents a random vector ranging from 0 to 1. The sign function is applied to the difference between $\vec{r}$ and 0.5, determining whether it is positive or negative. This sign determines the direction in which the exploration or exploitation will occur. By utilizing equation (9) for equation (7), equation (10) is extracted.

$$\vec{F} = a_1 \text{sign}(\vec{r} - 0.5) \times [\exp^{-\vec{\lambda} t} - 1]. \tag{10}$$

2.6 Generation rate (G)

The generation rate is a crucial parameter in the proposed algorithm, as it significantly impacts the quality of solutions by enhancing the exploitation phase. In the context of engineering applications, various strategies can be employed to represent the generation rate as a function of time. One such strategy involves utilizing a first-order exponential decay process to represent the generation rate [22]. The following equation defines this representation:

$$G = G_0 e^{-k(t - t_0)}, \tag{11}$$

where $G(t)$ represents the generation rate at time t, G_0 denotes the initial generation rate, and λ represents the decay rate parameter. By incorporating this exponential decay process, the generation rate can be appropriately modeled over time. In the EO, the equations employed to reformulate the generation rate are formulated as follows:

$$G = G_0 e^{-\lambda(t - t_0)} = G_0 F. \tag{12}$$

Subject to:

$$G_0 = \text{GCP}(C_{\text{eq}} - \lambda C), \tag{13}$$

$$\text{GCP} = \begin{cases} 0.5 r_1 & r_2 \geqslant \text{GP}, \\ 0 & r_2 < \text{GP}, \end{cases} \tag{14}$$

where r_1 and r_2 represent random numbers generated between 0 and 1. The generation rate control parameter (GCP) vector, obtained from equation (14), is used to compute the GCP variable. The GCP variable contributes to the updating process, influencing the generation rate control parameter.

A considerable number of particles in the EO utilize the generation concept to update their states. The selection of these particles is determined by a term called generation probability (GP), which is calculated using equations (13) and (14). The decision-making process based on equation (14) depends on the particle's level. If the GCP is zero, the G is assigned zero, and all the decision variables of these particles are updated without involving G. To strike a balance between exploration and exploitation, the GP is set to 0.5. This value ensures a good trade-off between exploring new solutions and exploiting promising ones. The updating rule of EO is applied as follows:

$$C = C_{\text{eq}} + (C - C_{\text{eq}}). F + \frac{G}{\lambda V}(1 - F). \tag{15}$$

As indicated in equation (15), the updating process for the concentrations of the particles in the EO involves three terms:

(1) The first term corresponds to the equilibrium concentration, which is randomly selected from the elite equilibrium pool. This pool comprises the top five solutions or equilibria obtained during the optimization process.

(2) The second term serves as an exploratory operator that helps guide the particles toward the optimal point in the search space. It contributes to the exploration of the solution space.
(3) The third term acts as an exploitation operator that enhances the quality of solutions. It is primarily controlled by the generation rate (as described in equation (12)). The generation rate influences the trade-off between exploration and exploitation.

The global and local search behavior is mainly governed by several parameters, including the concentrations in particles and equilibrium candidates, the turnover rate (λ), and the sign relationship between the second and third terms. When the signs of these terms are the same, it promotes global search by increasing the diversity. On the other hand, when the signs are opposite, it facilitates local search by reducing the diversity. By adjusting these parameters, the EO can strike a balance between global and local search, leading to effective exploration and exploitation in the optimization process. Figure 1 shows the movements of the equilibrium candidates.

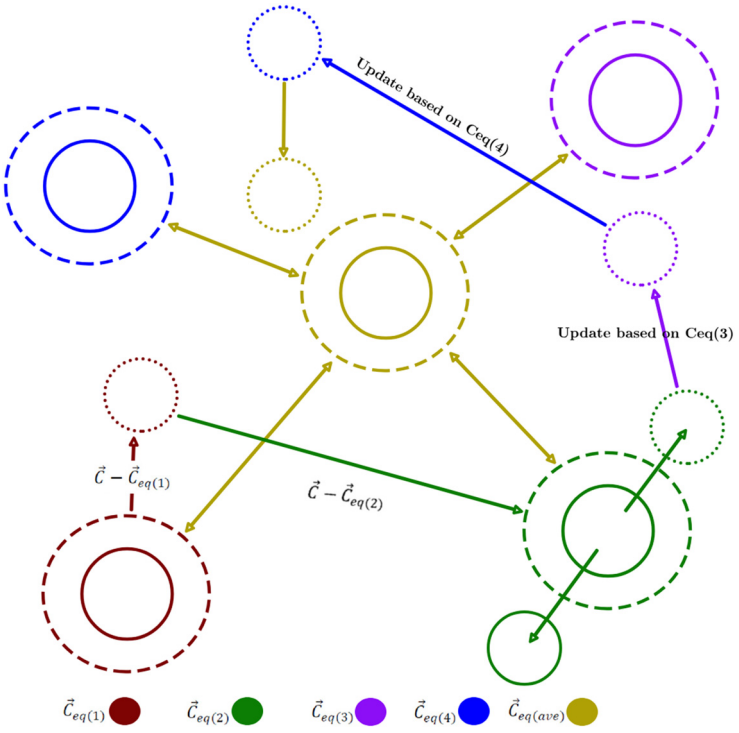

Figure 1: Equilibrium candidates' collaboration in updating a particles' concentration [21]. Source: Created by the authors.

Although the second term in equation (15) aims to target solutions from search space regions that are distant from the equilibrium candidates, and the third term extensively explores the search space region that includes the equilibrium candidates, and it is important to note that this behavior is not always guaranteed. Small changes made to the denominator of the third term can result in increased variations, which can contribute to the exploration of certain dimensions. The second term in equation (15), represented by $C_1 - C_{eq}$, and the third term, represented by $C_{eq} - \lambda \cdot C_1$, are influenced by the generation rate terms described in equations (13) and (14). The variation in these terms is governed by the value of the generation rate parameter λ, which can vary depending on the dimension.

Interestingly, high variation is more pronounced in dimensions where λ has smaller values. This mechanism is analogous to the mutation operator commonly observed in evolutionary-inspired algorithms. It allows for increased exploration in dimensions that may require more attention or have not been adequately explored, promoting the search for potentially better solutions in the optimization process.

2.7 Particle's memory saving

To enhance the performance of the EO and enable particles to track their trajectory in the search space, memory-saving procedures have been incorporated. In each iteration, the fitness value of a particle is compared to its fitness value in the previous iteration. If the current fitness value is better, it replaces the previous value, thus preserving the particle's best position so far. This mechanism reinforces the exploitation capability of the EO, as particles are able to retain their best-known solution. However, it is important to note that this mechanism can also introduce a potential challenge of stagnation in local minima if the algorithm does not perform sufficient global search. In such cases, the EO may become trapped in local optima and struggle to escape to potentially better solutions in other areas of the search space.

2.8 Exploration ability of EO

The exploitation task in the EO is achieved through the utilization of various parameters and mechanisms, including:

- a_1 is a parameter in the EO algorithm that plays a crucial role in controlling the exploration capability. It determines the distance between a new position and the equilibrium candidate. A higher value of a_1 increases the exploration ability of the EO algorithm.
- sign$(r - 0.5)$ is employed to control the trajectory of exploration. The variable r is generated randomly with a uniform distribution between 0 and 1.
- GP parameter utilizes the generation rate as a probability for contributing to the concentration updating process. The GP value determines the extent to which the generation rate term influences the exploration performance during optimization. When GP is set to one, it indicates that the generation rate term has a high contribution to the exploration performance. Conversely, when GP is set to zero, it implies that the generation rate term will always be contributing to the optimization process. This increases the likelihood of the algorithm getting stuck in local optima, as exploitation is prioritized over exploration.
- The equilibrium pool consists of five particles. The selection of these five particles is based on a slightly random criterion, which has been determined through initial experiments.

2.9 Exploitation ability of EO

The exploitation task is obtained utilizing the following parameters and mechanisms:

- a_2 is responsible for the exploitation task, specifically in determining the extent of exploitation. It governs the amount of deep search conducted around the best solution found so far.
- sign$(r - 0.5)$ controls the direction of exploitation and drives the local search in a specific direction. The variable r is randomly generated from a uniform distribution between 0 and 1.
- *Memory saving* is a memory parameter that keeps track of the best particles found so far during the optimization process.
- *Equilibrium pool* at the end of iterations. The equilibrium candidates are becoming more closer to each other.

The EO pseudocode in Algorithm 1 shows a comprehensive overview of the EO steps.

Algorithm 1 EO pseudocode

Initialize N (population size), Iter_{Max} (maximum number of generations), f (objective function), a_1, a_2, and GP
Initialize population $\mathbf{X}$ with N individuals
for iter ← 1 to Iter_{Max} **do**
  Calculate fitness for each individual in $\mathbf{X}$
  Sort individuals in $\mathbf{X}$ based on fitness
  for i ← 1 to N **do**
    Assign C_1, C_2, C_3, C_4 to the best four candidate
    $C_{\text{avg}} = \frac{C_1 + C_2 + C_3 + C_4}{4}$
    Construct the equilibrium pool
    Construct F, GCP, G_0, G
    Update concentrations
  end for
end for = 0

3 Proposed method

This section presents the main contribution of this work. The proposed method includes five phases, which are presented in Figure 2 and thoroughly discussed below.

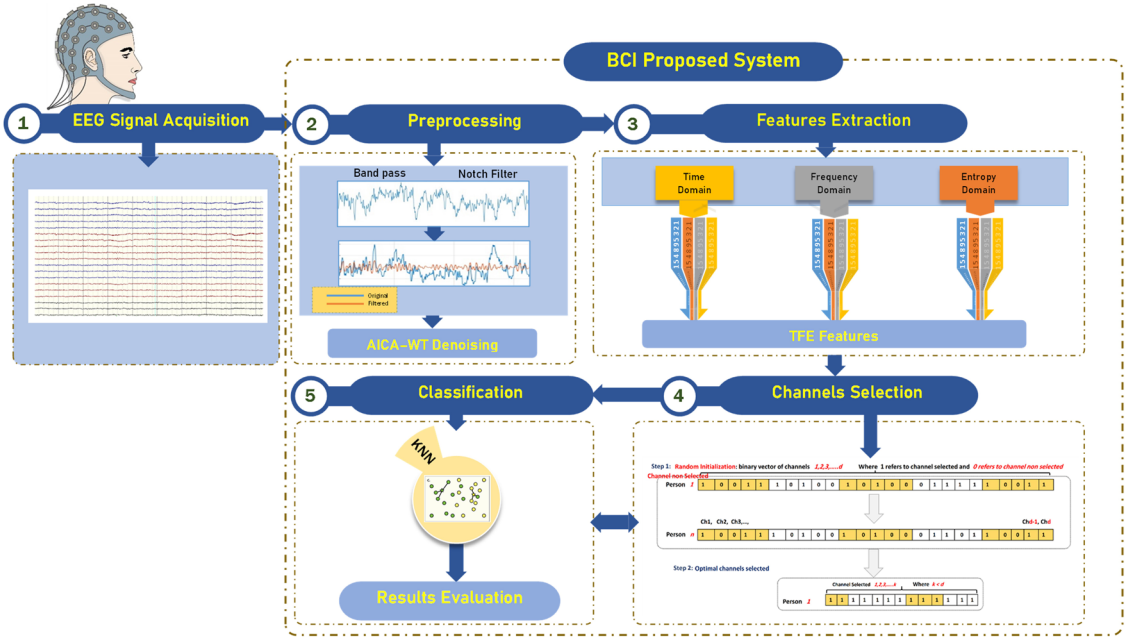

Figure 2: A proposed method for EEG channel selection. Source: Created by the authors.

3.1 Phase I: EEG signal acquisition

The EEG data of poststroke patients with hemiparesis of the upper extremities was studied. This study involved three poststroke patients treated with the recoveriX system (g.tec medical engineering GmbH), with a mean age of 22 years (SD = 4.582). Each participant got BCI-based MI training for three months, with

two training sessions each week (for a total of 25 training sessions). The study team conducted and analyzed two assessments (pre- and posttraining). The pretraining evaluation was scheduled 30–35 days prior to the intervention, whereas the post-training evaluation was conducted a few days after the intervention (see Figure 2). The Ethikkommission des Landes Oberosterreich in Austria ($\#D - 42 - 17$) authorized this study protocol, and each patient signed an informed consent form prior to the preassessment. Finally, this dataset is captured with a sample rate of 256 Hz. According to system indications for a MI mental task, the patients were instructed to visualize dorsal wrist movement. Before and after EEG neurorehabilitation, the patients participated in 25 MI-based BCI sessions with follow-up evaluation visits to measure the functional changes. Each session consisted of 240 MI repetitions with both hands and broken down into three 80-trial runs. Each session lasted approximately 1 h, including the time required for setup and cleanup. The MI-based BCI tasks were illustrated with randomized inter-trial intervals in a pseudo-random order.

Utilized were EEG caps with sixteen active electrodes from g.Nautilus PRO, g.tec medical engineering GmbH, Austria, based on the international 10–20 system.

3.2 Phase II: Preprocessing

Each channel of the recorded EEG dataset initially used two standard filters. First, a bandpass filter (BPF) with frequencies between (8 and 30 Hz) was used to confine the band of the recorded EEG dataset, [23], and second, a butter-worth (BW) notch filter at (50 Hz) was used to reduce the noise from power line interference. (ICs) $s(t) = [s_1(t), \ldots, s_n(t)]$ utilizing the *FastICA* algorithm proposed by [24]. The set $s(t)$ of n unknown components that were linearly mixed by within matrix A and $x(t)$ is the set of n observations where $x(t) = [x_1(t), \ldots, x_n(t)]$ [25–27], represents the EEGs and are related to $s(t)$, t is the time, the ICA equation is calculated as follows:

$$x(t) = As(t), \tag{16}$$

then, three metrics were used to evaluate the artifactual components ICs: Kurtosis (Kurt), skewness (Skw), and sample entropy (SampEn). If these parameters surpassed the ±1.2 threshold for each IC, the IC was marked as critical and denoised using WT. The practical value of the threshold is determined through trial and error and previous research [28–30]. The threshold value of ±1.2 is not a drawback of AICA-WT technique as the artifactual ICs will not be rejected but will be denoised using the WT technique. As a result, WT denoised the marked ICs before returning the enhanced components to the original EEG dataset [31,32].

3.3 Phase III: EEG features extraction

Three different feature extraction techniques are used in this work. These techniques include time domain features, entropy features, and frequency domain features as extracted in [7].

3.4 Phase IV: EEG channel selection using EO optimizer

This phase is the main contribution of this work, and it includes several steps to achieve the optimal subset of the EEG channel, which can provide the highest accuracy rate. The following steps represent how can we adapt the EO optimizer for the EEG channels selection problem.

- **Step 1: EO parameters initialization for EEG channel selection.** In this step, the EO parameters are initialized with initial values. These parameters are the number of microbats (solutions) (N), maximum number of iterations ($\mathrm{Max}_{\mathrm{Itr}}$), max ($C_{\max}$) and min ($C_{\min}$) frequency range, and the bandwidth range (ε) in the range $[-1, 1]$.

Also in this step, the EO population memory for the EEG channel selection problem should be Initialized. The EO solutions are randomly generated in this step using equation (17), considering the EO algorithm and particular optimization problem parameters and constraints.

$$\mathrm{EEGsol}_i^j = C_{\min} + r_i \times (C_{\max} - C_{\min}), \tag{17}$$

where $\forall i = 1, 2, \ldots, d$ d refers to the total number of the EEG channels, $\forall j = 1, 2, \ldots, N$, and r_i is a random number between 0 and 1. The produced solutions together generate the population, as shown in equation (19) and are stored in the EO memory (EOM) in the ascending order on the basis of their fitness values. The best solution with the fittest values is assigned to $\mathrm{EEGsol}^{\mathrm{Gbest}}$ and stored in the first position of EEGEOM.

$$\vec{C}_{\mathrm{eq,pool}} = \{\vec{C}_{\mathrm{eq}(1)}, \vec{C}_{\mathrm{eq}(2)}, \vec{C}_{\mathrm{eq}(3)}, \vec{C}_{\mathrm{eq}(4)}, \vec{C}_{\mathrm{eq}(\mathrm{ave})}\}, \tag{18}$$

$$\mathrm{EEGEOM} = \begin{bmatrix} \mathrm{EEGsol}_1^1 & \mathrm{EEGsol}_2^1 & \cdots & \mathrm{EEGsol}_d^1 \\ \mathrm{EEGsol}_1^2 & \mathrm{EEGsol}_2^2 & \cdots & \mathrm{EEGsol}_d^2 \\ \vdots & \vdots & \cdots & \vdots \\ \mathrm{EEGsol}_1^N & \mathrm{EEGsol}_2^N & \cdots & \mathrm{EEGsol}_d^N \end{bmatrix}, \tag{19}$$

Table 1: The performance of metaheuresitic algorithms using accuracy measure

Datasets	Measure	AOA	EO	GWO	SSA	WSO
ConvFuzEn	AVG	0.9465625	**0.953020833**	0.95171875	0.381510417	0.95046875
	STD	0.008132712	0.001945684	0.002821381	0.492528037	0.004133622
FDF1	AVG	0.96859375	**0.973489583**	0.972864583	0.4865625	0.972395833
	STD	0.002516463	0.000164702	0.00079369	0.512881943	0.001820849
FDF2	AVG	0.7615625	**0.771458333**	0.770052083	0.384947917	0.767239583
	STD	0.010193796	0.001509518	0.003868451	0.405771802	0.003846573
FuzEn	AVG	0.95015625	0.9571875	0.953802083	**0.958854167**	0.955677083
	STD	0.004678167	0.001898642	0.005109302	1.17028×10^{-16}	0.002760908
HFD	AVG	0.98609375	**0.990989583**	0.98984375	0.792864583	0.990052083
	STD	0.003699587	0.000886947	0.001257932	0.417876935	0.000866318
HjAc	AVG	0.969270833	**0.97140625**	0.969947917	0.699635417	0.969739583
	STD	0.002598373	0.000295649	0.001736979	0.440473119	0.001795008
HjComp	AVG	0.93109375	**0.941875**	0.938802083	0.658333333	0.9375
	STD	0.006701704	0.001824156	0.004455079	0.454294866	0.003201231
HjMo	AVG	0.974739583	**0.976458333**	0.975729167	0.585416667	0.9759375
	STD	0.00249481	0.000912078	0.001790805	0.503846544	0.001271042
Hur	AVG	0.603385417	**0.623177083**	0.618385417	0.436302083	0.613125
	STD	0.010503831	0.006584646	0.009071243	0.301101839	0.01163013
ImpEn	AVG	0.940208333	0.949270833	0.94671875	**0.949479167**	0.94421875
	STD	0.004485756	0.000658808	0.002832044	0	0.007715251
Kur	AVG	0.645625	**0.662291667**	0.658229167	0.417447917	0.66046875
	STD	0.010867556	0.001537218	0.006794386	0.321559578	0.003051311
MFEmu	AVG	0.8675	**0.8825**	0.879479167	0.53046875	0.877395833
	STD	0.007845993	0.005335259	0.00922331	0.456555253	0.008829281
RCMFEmu	AVG	0.822864583	**0.839010417**	0.836666667	0.8421875	0.833958333
	STD	0.015868948	0.009686349	0.004043313	1.17028×10^{-16}	0.009643781
SampEn	AVG	0.876197917	0.893125	0.88703125	**0.894270833**	0.88875
	STD	0.007914268	0.003623443	0.008081593	0	0.005306937
Skw	AVG	0.723958333	**0.737916667**	0.73734375	0.456458333	0.731875
	STD	0.006660877	0.001850405	0.002863794	0.362706828	0.007642045
TsEn	AVG	0.7865625	**0.799635417**	0.796927083	0.5846875	0.79859375
	STD	0.005917058	0.001152914	0.002282838	0.353137137	0.002303866

Bold values indicates the best results.

• **Step 2: EO population intensification.** Now, all microbats EEGsol will change their position considering by a frequency f generated randomly, as shown in equations (20) and (21). Accordingly, the EO positions will be updated using equation (22).

$$f_i = f_{\min} + (f_{\min} - f_{\max}) \times R, \tag{20}$$

$$v_i^{'j} = v_i^j + (\text{EEGsol}_i^j - \text{EEGsol}_i^{\text{Gbest}}) \times f_i, \tag{21}$$

$$\text{EEGsol}_i^{'j} = \text{EEGsol}_i^j + v_i^{'j}, \tag{22}$$

Notable that the microbats are updating their locations to be closer to the global best ($\text{EEGsol}^{\text{Gbest}}$). Thus, the new position of the microbats intensifies the position with a direction to $\text{EEGsol}^{\text{Gbest}}$.

Figure 3: The first column of figures presents the frequency domain, the second column of figures presents the time domain, and the third column presents the entropy domain. Source: Created by the authors.

• **Step 3: EO population diversification.**

In this step, the microbats positions are updated based on random parameters in attempting to find better global solutions. A new solution is selected from the BM based on a selection method and assigned to $\text{EEGsol}^{\text{best}}$. Subsequently, the current solution is updated using the $\text{EEGsol}^{\text{best}}$, as follows:

$$\text{EEGsol}_i^{\prime j} = \text{EEGsol}^{\text{best}} + \varepsilon \times A_j', \tag{23}$$

where A' is the loudness average. As Steps 2 and 3 are two contradictory steps, EO algorithm will choose one of them for execution at a time. This selection is based on the following equation:

$$\text{EEGsol}^{\prime j} = \begin{cases} \text{EEGsol}^{\text{best}} + \varepsilon \times A_j' & \text{if } r_j \le R \\ \text{EEGsol}^{j} + v'^{j} & \text{otherwise} \end{cases}, \tag{24}$$

• **Step 4: EEGBM update.** The position of the microbats in the EEGBM will be updated in this step if the new location is fitter than the old one and $R \le A_j$. Moreover, $\text{EEGsol}^{\text{Gbest}}$ will be updated if the new BM contains a solution with a better fitness value. Subsequently, r_j and A_j values will be updated in accordance with equations (25) and (26).

$$r_j = r_j^0(1 - e^{(-\gamma \times \text{Itr})}), \tag{25}$$

$$A_j = \alpha \times A_j, \tag{26}$$

where itr denotes the current iteration number.

• **Step 5: Stop criterion.** Steps 2, 3, and 4 will be repeated until the algorithm reach the stop criterion.

Algorithm 2 EO optimizer for EEG channel selection

Step 1: EO Parameters Initialization for EEG channel selection.
Initialize EO parameters: number of solutions (N), maximum iterations (Max_{Itr}), $C_{\max}$, $C_{\min}$, and ε.
Generate initial EO population using equation (19).
while $t \le \text{Max}_{\text{Itr}}$ **do**
  for each solution **do**
    Calculate the fitness values.
    Store population in *EEGEOM* and sort by fitness. Assign the best solution to $\text{EEGsol}^{\text{Gbest}}$.
    Step 2: EO Population Intensification.
    Generate frequency using equation (20).
    Update velocity using equation (21).
    Update position using equation (22).
  end for
  Step 3: EO Population Diversification.
  Select a new solution from BM and assign to $\text{EEGsol}^{\text{best}}$.
  Update position using equation (23).
  if $r_j \le R$ **then**
    Select solution using equation (24).
  end if
  Step 4: EEGBM Update.
  Replace the new solution with the old one if better.
  Update positions in EEGBM and $\text{EEGsol}^{\text{Gbest}}$.
  Step 5: Stop criterion.
  Repeat Steps 2, 3, and 4 until the stop criterion is reached.
end while

3.5 Phase V: Classification and performance measures

In this work, the k-nearest neighbor classifier is used. The performance of the proposed method and the optimal solution of the EO optimizer for the EEG channel selection problem was evaluated using the values of average classification accuracy. The overall average accuracy is computed using the following equation:

$$\text{Accuracy} = \frac{x}{N} \times 100, \tag{27}$$

where x refers to the number of correctly classified input data points and N refers to the total number of attributes.

4 Experiments and results

This section thoroughly explains the performance of the proposed method (EO) of EEG channels for stroke patient rehabilitation. Since the proposed approach is non-deterministic, the mean accuracy rate over 30 runs is computed to avoid biased results. The experiments use a with shed light on the stability of the algorithms by computing the best, worst, and mean accuracy. Moreover, a statistical test is adopted based on the

Table 2: The performance of metaheuristic algorithms using F-score

Datasets	Measure	AOA	EO	GWO	SSA	WSO
ConvFuzEn	AVG	0.946832119	**0.953262875**	0.951965442	0.781608129	0.950709208
	STD	0.008037741	0.001961691	0.00278043	0.572937211	0.004114336
FDF1	AVG	0.968662732	**0.973583625**	0.972924388	0.486589247	0.972468665
	STD	0.002505445	0.000136019	0.000807642	0.59527502	0.001817221
FDF2	AVG	0.765848181	**0.77571447**	0.77432163	0.386776463	0.771254412
	STD	0.010123323	0.001644672	0.003906705	0.700487328	0.003934393
FuzEn	AVG	0.950170416	0.957082222	0.95375705	**0.958786426**	0.955608431
	STD	0.004606085	0.001911391	0.005059211	2.34056×10^{16}	0.002733277
HFD	AVG	0.986108074	**0.991017833**	0.989860367	0.592892143	0.990072949
	STD	0.003696918	0.000898313	0.001271455	0.268657436	0.000874651
HjAc	AVG	0.969318828	**0.971463482**	0.970000214	0.499667405	0.969792696
	STD	0.002612324	0.00029782	0.001739281	0.339637634	0.001789194
HjComp	AVG	0.931312129	**0.941969319**	0.938955013	0.858440607	0.937689597
	STD	0.006709363	0.001783278	0.004359095	10.477816871	0.003116884
HjMo	AVG	0.974769004	**0.976496465**	0.975763734	0.185438715	0.975981147
	STD	0.002485038	0.000904107	0.001780518	0.561725728	0.001266756
Hur	AVG	0.608918953	**0.649550373**	0.624409709	0.641186655	0.619313624
	STD	0.011240543	0.00715559	0.009813872	0.627739709	0.011929772
ImpEn	AVG	0.940307653	0.949305087	0.946766788	**0.949506691**	0.944281792
	STD	0.004465068	0.000637528	0.002830913	1.17028×10^{16}	0.007672175
Kur	AVG	0.648149312	**0.664929412**	0.66087958	0.619040465	0.663065177
	STD	0.01134061	0.001512144	0.006844287	0.649279043	0.003143289
MFEmu	AVG	0.866781958	**0.882165437**	0.879194415	0.130260645	0.877019968
	STD	0.007877488	0.005344748	0.009145957	0.609215553	0.008903859
RCMFEmu	AVG	0.82458336	**0.840606199**	0.838235121	0.840122207	0.835569826
	STD	0.015795335	0.009641837	0.004079127	1.17028×10^{16}	0.009677939
SampEn	AVG	0.877661124	0.894495796	0.888342549	**0.895641487**	0.890072641
	STD	0.007788074	0.003622995	0.008088093	0	0.005291155
Skw	AVG	0.725045287	**0.738665975**	0.737843081	0.65697223	0.733027897
	STD	0.006244957	0.001483467	0.002956336	0.626904761	0.007365607
TsEn	AVG	0.787619014	**0.800884534**	0.798068436	0.385750353	0.799813432
	STD	0.005803214	0.001250456	0.002407282	0.388641437	0.002314258

Bold values indicates the best results.

Table 3: The performance of metaheuristic algorithms using fitness values

Datasets	Measure	AOA	EO	GWO	SSA	WSO
ConvFuzEn	AVG	0.061403125	0.055634375	0.056610938	**0.055007813**	0.057723438
	STD	0.007257729	0.001611812	0.00244424	**0.000556939**	0.003674656
FDF1	AVG	0.038967188	**0.035057813**	0.035614063	0.035410938	0.035953125
	STD	0.002089359	$\mathbf{3.45874 \times 10^{-5}}$	0.000588337	0.000739475	0.001435366
FDF2	AVG	0.244490625	**0.23525625**	0.236273438	0.23531875	0.239370313
	STD	0.009661755	**0.001904573**	0.003598082	0.002004825	0.003641151
FuzEn	AVG	0.057595313	0.051321875	0.054110938	**0.050734375**	0.052879688
	STD	0.004448255	0.001988604	0.004628421	$\mathbf{7.31424 \times 10^{-18}}$	0.002602667
HFD	AVG	0.021142188	**0.017670313**	0.017929688	0.017673438	0.018223438
	STD	0.003233074	0.00032371	0.000810436	**0.000287588**	0.000596123
HjAc	AVG	0.038359375	**0.036557813**	0.037814063	0.036601563	0.038270313
	STD	0.002388667	0.000161886	0.001434864	**0.000149189**	0.001553639
HjComp	AVG	0.076529688	0.06679375	0.069710938	**0.066351563**	0.070875
	STD	0.006186708	0.001553739	0.004078715	**0.000815275**	0.002868747
HjMo	AVG	0.032945313	0.03149375	0.031965625	**0.0314125**	0.032259375
	STD	0.001881633	0.000663902	0.001321538	**0.000566594**	0.001118645
Hur	AVG	0.401023438	0.382242188	0.386735938	**0.379501563**	0.39188125
	STD	0.009937801	0.006231062	0.008578324	**0.002969576**	0.011241862
ImpEn	AVG	0.06781875	0.060159375	0.062123438	**0.060015625**	0.064723438
	STD	0.004283139	0.000454577	0.002360834	**0**	0.007261355
Kur	AVG	0.35964375	0.34370625	0.347478125	**0.342984375**	0.345635938
	STD	0.010146392	0.001521846	0.006322892	$\mathbf{5.85139 \times 10^{-17}}$	0.00298706
MFEmu	AVG	0.1397375	0.1256375	0.128440625	**0.123328125**	0.130565625
	STD	0.007330665	0.005110635	0.00869835	$\mathbf{1.46285 \times 10^{-17}}$	0.008439554
RCMFEmu	AVG	0.184364063	0.169192188	0.1710125	**0.166234375**	0.17388125
	STD	0.015176256	0.009211567	0.003535295	$\mathbf{2.92569 \times 10^{-17}}$	0.009034791
SampEn	AVG	0.131189063	0.11568125	0.121151563	**0.114671875**	0.119575
	STD	0.007436557	0.003191924	0.007517576	**0**	0.00486888
Skw	AVG	0.28153125	**0.2684**	0.268717188	0.271054688	0.27450625
	STD	0.006178339	0.002133042	0.002680086	**0.001421565**	0.007256101
TsEn	AVG	0.219428125	0.207610938	0.209542188	**0.207375**	0.208517188
	STD	0.005693121	0.0007461	0.001713788	$\mathbf{2.92569 \times 10^{-17}}$	0.001931757

Bold values indicates the best results.

classification accuracy motor/imaging EEG dataset using the sum of ranks of the meta-heuristic algorithms. Three types of EEG features such as time domain features, frequency domain features, and entropy domain features are extracted. Also, the performance results of the proposed method are evaluated using a statistical test to show the significance of the proposed method compared with other meta-heuristic algorithms. The performance of the proposed method (EO-EEG) is evaluated using several measures such as accuracy, F-score, MCC, fitness values, FPR, Kappa, precision, sensitivity, and EEG channel selection. The formula of these measures as fellows:

$$\text{Accuracy} = \frac{\text{TP} + \text{TN}}{\text{TP} + \text{TN} + \text{FP} + \text{FN}}, \tag{28}$$

$$\text{Precision} = \frac{\text{TP}}{\text{TP} + \text{FP}}, \tag{29}$$

$$\text{Recall} = \frac{\text{TP}}{\text{TP} + \text{FN}}, \tag{30}$$

$$F1 = \frac{2*\text{Precision}*\text{Recall}}{\text{Precision} + \text{Recall}} = \frac{2*\text{TP}}{2*\text{TP} + \text{FP} + \text{FN}}, \tag{31}$$

Table 4: The performance of metaheuristic algorithms using FPR

Datasets	Measure	AOA	EO	GWO	SSA	WSO
ConvFuzEn	AVG	0.007633929	**0.00671131**	0.006897321	0.802641369	0.007075893
	STD	0.001161816	**0.000277955**	0.000403054	0.545783347	0.000590517
FDF1	AVG	0.004486607	**0.003787202**	0.003876488	0.501919643	0.003943452
	STD	0.000359495	$\mathbf{2.35289} \times 10^{-5}$	0.000113384	0.579115349	0.000260121
FDF2	AVG	0.0340625	**0.03264881**	0.032849702	0.516436012	0.033251488
	STD	0.001456257	**0.000215645**	0.000552636	0.563813758	0.00054951
FuzEn	AVG	0.007120536	0.006116071	0.006599702	**0.005877976**	0.006331845
	STD	0.00066831	0.000271235	0.0007299	**0**	0.000394415
HFD	AVG	0.001986607	**0.001287202**	0.001450893	0.601019345	0.001421131
	STD	0.000528512	**0.000126707**	0.000179705	0.264373826	0.00012376
HjAc	AVG	0.004389881	**0.004084821**	0.004293155	0.614337798	0.004322917
	STD	0.000371196	$\mathbf{4.22356} \times 10^{-5}$	0.00024814	0.257825376	0.00025643
HjComp	AVG	0.00984375	**0.008303571**	0.00874256	0.905952381	0.008928571
	STD	0.000957386	**0.000260594**	0.00063644	0.445030152	0.000457319
HjMo	AVG	0.003608631	**0.003363095**	0.003467262	0.202083333	0.0034375
	STD	0.000356401	**0.000130297**	0.000255829	0.547400291	0.000181577
Hur	AVG	0.056659226	**0.053831845**	0.054516369	0.937671131	0.055267857
	STD	0.001500547	**0.000940664**	0.001295892	0.423142232	0.001661447
ImpEn	AVG	0.008541667	0.007247024	0.007611607	**0.007217262**	0.00796875
	STD	0.000640822	9.41154×10^{-5}	0.000404578	**0**	0.001102179
Kur	AVG	0.050625	**0.048244048**	0.048824405	0.940364583	0.048504464
	STD	0.001552508	**0.000219603**	0.000970627	0.421430051	0.000435902
MFEmu	AVG	0.018928571	**0.01678571**4	0.017217262	0.209933036	0.017514881
	STD	0.001120856	**0.00076218**	0.001317616	0.540644345	0.001261326
RCMFEmu	AVG	0.02530506	0.022998512	0.023333333	**0.022544643**	0.023720238
	STD	0.002266993	0.001383764	0.000577616	**0**	0.001377683
SampEn	AVG	0.017686012	0.015267857	0.016138393	**0.015104167**	0.015892857
	STD	0.00113061	0.000517635	0.001154513	$\mathbf{3.65712} \times 10^{-18}$	0.000758134
Skw	AVG	0.039434524	**0.037440476**	0.037522321	0.934791667	0.038303571
	STD	0.000951554	**0.000264344**	0.000409113	0.425360683	0.001091721
TsEn	AVG	0.030491071	**0.028623512**	0.029010417	0.630758929	0.028772321
	STD	0.000845294	**0.000164702**	0.00032612	0.24894273	0.000329124

Bold values indicates the best results.

$$\mathrm{MCC} = \frac{\mathrm{TP} \times \mathrm{TN} - \mathrm{FP} \times \mathrm{FN}}{\sqrt{(\mathrm{TP} + \mathrm{FP})(\mathrm{TP} + \mathrm{FN})(\mathrm{TN} + \mathrm{FP})(\mathrm{TN} + \mathrm{FN})}}, \tag{32}$$

$$\kappa = \frac{p_o - p_e}{1 - p_e}, \tag{33}$$

where κ represents the Kappa coefficient, p_o is the observed agreement, and p_e is the expected agreement by chance.

Also, the performance of the proposed method compares with four other metaheuristic algorithms: White shark optimizer (WSO) [33], grey wolf optimizer (GWO) [34], Salp swarm algorithm (SSA) [35], and arithmetic optimization algorithm (AOA) [36].

Table 1 presents the results of 16 EEG features in the time, frequency, and time–frequency domain features based on the accuracy measure. The averaging accuracy rate for 30 times is presented with the standard deviation of these runs (STD). According to Table 1, the performance results for several meta-heuristic algorithms such as AOA, EO, GWO, SSA, and WSO with several features have achieved different remarkable accuracy concerning mean accuracy and the number of channel selections. The EO algorithm achieves better results over all other metaheuristics, and the highest accuracy rate is obtained using the HFD feature, which equals 0.990989583. Moreover, the SSA algorithm achieved high accuracy with FuzEn, ImpEn, and SampEn features.

Table 5: The performance of metahurstic algorithms using Kappa

Datasets	Measure	AOA	EO	GWO	SSA	WSO
ConvFuzEn	AVG	0.755714286	0.785238095	0.779285714	**0.91547619**	0.773571429
	STD	0.037178114	**0.008894556**	0.012897741	0.691109456	0.018896557
FDF1	AVG	0.856428571	**0.878809524**	0.875952381	0.438571429	0.873809524
	STD	0.011503831	**0.000752923**	0.003628295	0.699982923	0.00832388
FDF2	AVG	**0.081103202**	0.042806742	0.048459095	0.024657655	0.059961228
	STD	0.038116862	**0.006287873**	0.015754147	0.136288611	0.015546211
FuzEn	AVG	0.772142857	0.804285714	0.788809524	**0.811904762**	0.797380952
	STD	0.021385907	0.008679507	0.023356807	$\mathbf{1.17028 \times 10^{-16}}$	0.012621294
HFD	AVG	0.936428571	0.958809524	0.953571429	**0.967380952**	0.95452381
	STD	0.016912399	**0.004054616**	0.005750546	0.125379355	0.00396031
HjAc	AVG	0.85952381	0.869285714	0.862619048	**0.880328599**	0.861666667
	STD	0.011878277	**0.001351539**	0.007940475	0.17170293	0.00820575
HjComp	AVG	0.685	**0.734285714**	0.720238095	0.30952381	0.714285714
	STD	0.03063636	**0.008339**	0.020366075	0.546676877	0.014634198
HjMo	AVG	0.88452381	0.892380952	0.889047619	**0.933333333**	0.89
	STD	0.011404848	**0.0041695**	0.008186538	0.639366826	0.005810478
Hur	AVG	**0.4481144**	0.419331913	0.426489861	0.093466812	0.434119247
	STD	0.014376709	**0.009963207**	0.013456421	0.695770548	0.016737844
ImpEn	AVG	0.726666667	0.768095238	0.756428571	**0.769047619**	0.745
	STD	0.020506315	0.003011693	0.012946486	$\mathbf{1.17028 \times 10^{-16}}$	0.03526972
Kur	AVG	0.382201214	0.352239695	0.359727127	**2.083783302**	0.355682954
	STD	0.01866199	**0.002929571**	0.01252643	2.70492186	0.005743432
MFEmu	AVG	0.394285714	0.462857143	0.449047619	**2.682142857**	0.43952381
	STD	0.035867397	**0.024389755**	0.042163702	0.855558258	0.04036243
RCMFEmu	AVG	0.190238095	0.264047619	0.253333333	**0.278571429**	0.240952381
	STD	0.072543764	0.044280451	0.018483716	**0**	0.044085855
SampEn	AVG	0.434047619	0.511428571	0.483571429	**0.516666667**	0.491428571
	STD	0.03617951	0.016564312	0.036944423	**0**	0.024260283
Skw	AVG	0.207128817	0.165304587	0.16707427	**0.978285056**	0.183566727
	STD	0.019269745	**0.005858243**	0.008981525	0.780784196	0.022710352
TsEn	AVG	0.030426582	0.084047619	0.071666667	**0.330954357**	0.079285714
	STD	0.018881128	**0.005270463**	0.010435829	0.468478741	0.010531958

Bold values indicates the best results.

Figures 3 and 4 show the results of the AOA, EO, GWO, SSA, and WSO using time, frequency, and time–frequency domain features.

Table 2 presents the results of 16 EEG features in the time, frequency, and time–frequency domain features based on the F-score measure. The averaging F-score for 30 times is presented with the standard deviation of these runs (STD). According to Table 2, the performance results for several meta-heuristic algorithms such as AOA, EO, GWO, SSA, and WSO with several features have achieved different remarkable accuracy concerning mean F-score and the number of channels selection. The EO algorithm achieves better results over all other metaheuristics and the highest accuracy rate is obtained using the HFD feature, which equals 0.9910171447. Moreover, the SSA algorithm achieved high accuracy with FuzEn, ImpEn, and SampEn features.

Table 3 presents the results of 16 EEG features in the time, frequency, and time–frequency domain features based on the fitness values measured. The averaging accuracy rate for 30 times is presented with the standard deviation of these runs (STD). The table proved the high performance of the EO compared to other algorithms in optimizing the AVG and STD of the fitness values in 5 and 2 datasets, respectively. However, the SSA obtained better AVG results in 11 datasets.

Table 4 presents the results of 16 EEG features in the time, frequency, and time–frequency domain features based on the FPR measure. The averaging accuracy rate for 30 times is presented with the standard deviation of these runs (STD). The table proved the high performance of the EO compared to other algorithms

Table 6: The performance of metaheuristic algorithms using MCC

Datasets	Measure	AOA	EO	GWO	SSA	WSO
ConvFuzEn	AVG	0.939347341	**0.946663478**	0.945198582	0.379016846	0.943782816
	STD	0.009158445	**0.002241815**	0.003163781	0.092680318	0.00466651
FDF1	AVG	0.964305674	0.969925947	0.969167685	**0.984721672**	0.968657033
	STD	0.002871647	**0.000143801**	0.000917599	0.124289896	0.00206237
FDF2	AVG	0.734109411	0.745714504	0.744099422	**0.871607889**	0.740410977
	STD	0.011812583	**0.001995119**	0.004616124	0.243522705	0.004635509
FuzEn	AVG	0.943171709	0.951080281	0.947252787	**0.953015539**	0.949381554
	STD	0.005244733	0.002165471	0.00579659	**0**	0.003126003
HFD	AVG	0.984167372	**0.989769057**	0.988446567	0.791903673	0.988689281
	STD	0.004217235	**0.001031477**	0.001450944	0.690815425	0.000996583
HjAc	AVG	0.965017054	**0.967459169**	0.965784959	0.685769502	0.965583864
	STD	0.00297191	**0.000337337**	0.001979203	0.768152447	0.002031469
HjComp	AVG	0.921806913	**0.933955064**	0.930494175	0.152661165	0.929037567
	STD	0.007610882	**0.00202897**	0.004981774	0.964850967	0.003551982
HjMo	AVG	0.971221813	**0.973198343**	0.972358398	0.583400475	0.972604871
	STD	0.00283458	**0.001029377**	0.00202778	0.079877743	0.001444611
Hur	AVG	0.557997135	0.582297592	0.575909351	**0.90851853**	0.570235277
	STD	0.013151705	**0.008649209**	0.011877299	0.133328484	0.013579275
ImpEn	AVG	0.931896666	0.942201166	0.939294532	**0.942435046**	0.936477377
	STD	0.005089189	0.000739592	0.003230427	$\mathbf{1.17028} \times 10^{-16}$	0.008763331
Kur	AVG	0.600128051	0.619048746	0.614409663	**0.880669505**	0.616957225
	STD	0.013198617	**0.001999947**	0.008063513	0.158727826	0.003637141
MFEmu	AVG	0.849362237	**0.86660842**	0.863183816	0.521040039	0.860853825
	STD	0.008929125	**0.005899206**	0.010314506	0.133549146	0.009888445
RCMFEmu	AVG	0.801639513	0.819953924	0.817078088	**0.823593547**	0.814263655
	STD	0.017695702	0.010709732	0.004716803	**0**	0.010923145
SampEn	AVG	0.861110567	0.879994606	0.873157448	**0.881304924**	0.875025846
	STD	0.008827063	0.004143589	0.009069253	**0**	0.005952573
Skw	AVG	0.687830704	0.703832676	0.702698219	**0.924302594**	0.697396054
	STD	0.006950396	**0.001703606**	0.003700277	0.132447917	0.008610743
TsEn	AVG	0.758770872	**0.773736077**	0.770427136	0.556405189	0.772684196
	STD	0.006723758	**0.001470839**	0.002878097	0.825601379	0.002321218

Bold values indicates the best results.

in optimizing the AVG and STD of the FPR in 12 datasets for both. However, the SSA obtained better AVG results in 4 datasets.

Table 5 presents the results of 16 EEG features in the time, frequency, and time–frequency domain features based on the Kappa measure. The averaging accuracy rate for 30 times is presented with the standard deviation of these runs (STD). The table proved the high performance of the EO compared to other algorithms in optimizing the AVG and STD of the Kappa in 2 and 12 datasets, respectively. However, the SSA obtained better AVG results in 12 datasets.

Table 6 presents the results of 16 EEG features in the time, frequency, and time–frequency domain features based on the MCC measure. The averaging accuracy rate for 30 times is presented with the standard deviation of these runs (STD). The table proved the high performance of the EO compared to other algorithms in optimizing the AVG and STD of the MCC in 7 and 12 datasets, respectively. However, the SSA obtained better AVG results in 9 datasets.

Table 7 presents the results of 16 EEG features in the time, frequency, and time–frequency domain features based on the precision measure. The averaging accuracy rate for 30 times is presented with the standard deviation of these runs (STD). The table proved the high performance of the EO compared to other algorithms in optimizing the AVG and STD of the precision in 11 and 12 datasets, respectively. However, the SSA obtained better AVG results in five datasets.

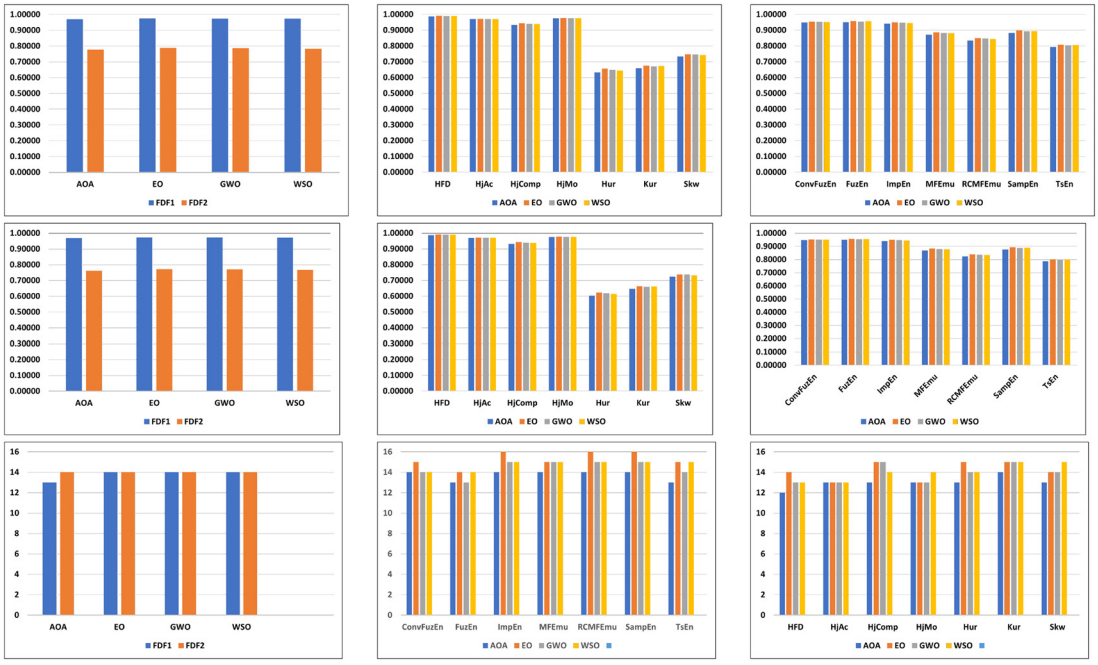

Figure 4: The first column of figures presents the frequency domain, the second column of figures presents the time domain, and the third column presents the entropy domain. Source: Created by the authors.

Table 7: The performance of metaheuristic algorithms using precision

Datasets	Measure	AOA	EO	GWO	SSA	WSO
ConvFuzEn	AVG	0.947574382	**0.953862614**	0.952626517	0.581865266	0.951422192
	STD	0.007814717	**0.001986904**	0.002681388	0.539809804	0.003979142
FDF1	AVG	0.969131193	**0.974078216**	0.973353101	0.486776274	0.972947509
	STD	0.00251532	5.78565×10^{-5}	0.000819799	0.540985395	0.001771388
FDF2	AVG	0.777299082	**0.788101902**	0.786663119	0.392506175	0.782691176
	STD	0.010771351	**0.0022001**	0.00447413	0.640356844	0.004587586
FuzEn	AVG	0.950557907	0.957319839	0.954001123	**0.959042388**	0.955856787
	STD	0.00443994	0.001872132	0.005029292	$\mathbf{2.34056} \times 10^{-16}$	0.002699225
HFD	AVG	0.98626347	**0.991164973**	0.989991221	0.19301551	0.990209463
	STD	0.003669237	**0.000930078**	0.001285091	0.425318805	0.000878051
HjAc	AVG	0.969638724	**0.971769916**	0.970293711	0.100791369	0.970197136
	STD	0.002591922	**0.000293894**	0.001717049	0.530495614	0.001742732
HjComp	AVG	0.932572045	**0.942950125**	0.939974539	0.259081343	0.938732933
	STD	0.00656308	**0.001696732**	0.004224153	0.511283914	0.002970771
HjMo	AVG	0.97498763	**0.976734979**	0.975989164	0.385599507	0.976214281
	STD	0.002455762	**0.000883197**	0.001744923	0.528791824	0.001252873
Hur	AVG	0.631834807	**0.655880272**	0.648704254	0.061230666	0.644303759
	STD	0.013620575	**0.009403382**	0.012893027	0.647817947	0.012373614
ImpEn	AVG	0.940811485	0.949777868	0.947243029	**0.949980005**	0.944850175
	STD	0.004394706	0.000639213	0.002814948	$\mathbf{2.34056} \times 10^{-16}$	0.007592979
Kur	AVG	0.658508714	**0.674711319**	0.670646916	0.026070393	0.672901919
	STD	0.012924055	**0.002280037**	0.007687313	0.687326935	0.003511738
MFEmu	AVG	0.87067588	**0.885600719**	0.882608337	0.332237439	0.8807807
	STD	0.00773912	**0.004712517**	0.008608719	0.574718734	0.008139463
RCMFEmu	AVG	0.833575219	0.849402726	0.846503171	**0.852565556**	0.84460488
	STD	0.014673512	0.008676349	0.004306568	**0**	0.009295083
SampEn	AVG	0.882655441	0.898257385	0.892619823	**0.899406767**	0.894028112
	STD	0.007435252	0.003634666	0.007583663	**0**	0.004998817
Skw	AVG	0.732786943	**0.747235759**	0.745455404	0.063631972	0.742213626
	STD	0.005462565	**0.001092764**	0.004153879	0.67142651	0.007618174
TsEn	AVG	0.793620133	0.806607237	0.803356089	**0.990913497**	0.806001889
	STD	0.006091045	**0.001581889**	0.003030186	0.559100199	0.001626563

Bold values indicates the best results.

Table 8: The performance of metaheuristic algorithms using sensitivity

Datasets	Measure	AOA	EO	GWO	SSA	WSO
ConvFuzEn	AVG	0.9465625	**0.953020833**	0.95171875	0.381510417	0.95046875
	STD	0.008132712	**0.001945684**	0.002821381	0.492528037	0.004133622
FDF1	AVG	0.96859375	**0.973489583**	0.972864583	0.4865625	0.972395833
	STD	0.002516463	**0.000164702**	0.00079369	0.512881943	0.001820849
FDF2	AVG	0.7615625	**0.771458333**	0.770052083	0.384947917	0.767239583
	STD	0.010193796	**0.001509518**	0.003868451	0.405771802	0.003846573
FuzEn	AVG	0.95015625	0.9571875	0.953802083	**0.958854167**	0.955677083
	STD	0.004678167	0.001898642	0.005109302	**0**	0.002760908
HFD	AVG	0.98609375	**0.990989583**	0.98984375	0.792864583	0.990052083
	STD	0.003699587	**0.000886947**	0.001257932	0.417876935	0.000866318
HjAc	AVG	0.969270833	**0.97140625**	0.969947917	0.699635417	0.969739583
	STD	0.002598373	**0.000295649**	0.001736979	0.440473119	0.001795008
HjComp	AVG	0.93109375	**0.941875**	0.938802083	0.658333333	0.9375
	STD	0.006701704	**0.001824156**	0.004455079	0.454294866	0.003201231
HjMo	AVG	0.974739583	**0.976458333**	0.975729167	0.585416667	0.9759375
	STD	0.00249481	**0.000912078**	0.001790805	0.503846544	0.001271042
Hur	AVG	0.603385417	**0.623177083**	0.618385417	0.436302083	0.613125
	STD	0.010503831	**0.006584646**	0.009071243	0.301101839	0.01163013
ImpEn	AVG	0.940208333	0.949270833	0.94671875	**0.949479167**	0.94421875
	STD	0.004485756	0.000658808	0.002832044	$\mathbf{1.17028} \times 10^{-16}$	0.007715251
Kur	AVG	0.645625	**0.662291667**	0.658229167	0.417447917	0.66046875
	STD	0.010867556	**0.001537218**	0.006794386	0.321559578	0.003051311
MFEmu	AVG	0.8675	**0.8825**	0.879479167	0.53046875	0.877395833
	STD	0.007845993	**0.005335259**	0.00922331	0.456555253	0.008829281
RCMFEmu	AVG	0.822864583	0.839010417	0.836666667	**0.8421875**	0.833958333
	STD	0.015868948	0.009686349	0.004043313	**0**	0.009643781
SampEn	AVG	0.876197917	0.893125	0.88703125	**0.894270833**	0.88875
	STD	0.007914268	0.003623443	0.008081593	**0**	0.005306937
Skw	AVG	0.723958333	**0.737916667**	0.73734375	0.456458333	0.731875
	STD	0.006660877	**0.001850405**	0.002863794	0.362706828	0.007642045
TsEn	AVG	0.7865625	**0.799635417**	0.796927083	0.5846875	0.79859375
	STD	0.005917058	**0.001152914**	0.002282838	0.353137137	0.002303866

Bold values indicates the best results.

Table 8 presents the results of 16 EEG features in the time, frequency, and time–frequency domain features based on the sensitivity measure. The averaging accuracy rate for 30 times is presented with the standard deviation of these runs (STD). The table proves the high performance of the EO compared to other algorithms in optimizing the AVG and STD of the sensitivity in 12 for both. However, the SSA obtained better AVG results in four datasets.

Table 9 presents the results of 16 EEG features in the time, frequency, and time–frequency domain features based on the number of EEG channel selection measure. The averaging accuracy rate for 30 times is presented with the standard deviation of these runs (STD). The presented results proved the high performance of the utilized EO algorithm compared with all the other algorithms by achieving the best results in most of the measurements and datasets.

5 Conclusions and future work

This work introduces a new technique to select relevant EEG channels for stroke patient's rehabilitation using a binary version of the EO, termed EO-EEG. The primary objective of the EO algorithm is to select the most

Table 9: The performance of metahurstic algorithms using No. Channel selected

Datasets	Measure	AOA	EO	GWO	SSA	WSO
ConvFuzEn	AVG	**14**	15	**14**	15	**14**
	STD	0.3498	0.6992	0.8755	**0**	0.1005
FDF1	AVG	**13**	14	14	15	14
	STD	0.9660	**0.31626**	0.47140	0.849	0.7888
FDF2	AVG	**14**	**14**	**14**	15	**14**
	STD	**0.0801**	0.6992	0.42163	0.84986	0.1595
FuzEn	AVG	**13**	14	**13**	16	14
	STD	0.63245	0.674948558	0.6999	**0**	0.6999
HFD	AVG	**12**	14	13	15	13
	STD	0.22927	0.3333	0.1737	**0.0801**	0.96603
HjAc	AVG	**13**	**13**	**13**	14	**13**
	STD	0.4832	**0.4216**	0.5676	0.51779	0.94898
HjComp	AVG	**13**	15	15	15	14
	STD	0.82327	0.42163	0.6992	**0**	0.6992
HjMo	AVG	**13**	**13**	**13**	**13**	14
	STD	1.3374	0.7378	0.8232	0.48304	**0.0801**
Hur	AVG	**13**	15	14	15	14
	STD	0.9660	0.48304	0.67494	**0.31622**	0.6324
ImpEn	AVG	**14**	16	15	16	15
	STD	0.63245	0.3162	0.05403	**0**	0.03279
Kur	AVG	**14**	15	15	15	15
	STD	0.10035	**0**	0.6999	0.3166	0.42161
MFEmu	AVG	**14**	15	15	15	15
	STD	0.8232	0.31626	0.65899	**0**	0.67458
RCMFEmu	AVG	**14**	16	15	16	15
	STD	0.9663	0.67458	0.87556	**0**	0.91893
SampEn	AVG	**14**	16	15	16	15
	STD	0.9183	0.6324	0.9996	**0**	0.8755
Skw	AVG	**13**	14	14	15	15
	STD	**0.03279**	0.48392	0.5676	0.47121	0.84986
TsEn	AVG	**13**	15	14	15	15
	STD	0.6667	0.63245	0.9663	**0**	0.6999

Bold values indicates the best results.

informative EEG channels that offer a higher accuracy rate, ultimately enhancing the efficacy of BCI systems in stroke rehabilitation.

To validate the proposed method (EO-EEG), an EEG dataset was utilized, consisting of recordings from eight poststroke patients with hemiparesis of the upper extremities. The EEG data were captured using g.Nautilus PRO EEG caps equipped with 16 active electrodes from g.tec Medical Engineering GmbH, Austria. The performance of EO-EEG was rigorously evaluated using several metrics, including accuracy, F-score, MCC, FIT, FPR, Kappa, precision, sensitivity, and EEG channel selection. These comprehensive measures ensure a robust assessment of the proposed method's effectiveness. Furthermore, The EO-EEG method incorporates various EEG feature extraction techniques, spanning the time, frequency, and entropy domains. It compares the performance of the O algorithm against four other prominent metaheuristic algorithms: AOA, GWO, SSA, and WSO. The evaluation focused on both the accuracy rate and the number of channels selected, demonstrating that EO-EEG outperforms other methods.

A notable achievement of the proposed method is its ability to reduce the number of EEG channels while maintaining a high accuracy rate, with the highest accuracy rate achieved being 99%. This reduction in channels simplifies the EEG setup, enhances user comfort, and reduces computational load, making the method highly practical for clinical use.

In terms of future work, several challenges remain to be addressed as follows:

- The current version of the EO algorithm can struggle with generating new solutions that enhance accuracy, often becoming trapped in local minima. To overcome this limitation, modifications to the EO algorithm's mechanism or hybridization with another metaheuristic algorithm will be explored to improve its capability in finding the optimal solution.
- The current EO algorithm primarily focuses on maximizing accuracy without factoring in the number of EEG channels as part of the objective function. Future work will involve developing a multiobjective version of the EO algorithm that simultaneously considers both the highest accuracy and the lowest number of EEG channels. This approach will further optimize the balance between accuracy and efficiency, enhancing the practical applicability of the method in stroke rehabilitation.
- EO, like many other metaheuristic algorithms, can sometimes converge prematurely to suboptimal solutions. This happens when the algorithm gets trapped in local minima, reducing its ability to explore the global search space effectively. To address this, hybridization with other optimization techniques could be explored. Combining EO with methods like simulated annealing or genetic algorithms could enhance its exploration capabilities and avoid premature convergence.

Funding information: This work was supported by the Deanship of Research and Graduate Studies (DRG) at Ajman University, Ajman, UAE (Grant No. 2022-IRG-ENIT-7).

Author contributions: Conceptualization: M.A.A.-B. and Z.A.A.A.; methodology: M.A.A.-B., Z.A.A.A., and S.N.M.; software: M.A.A.-B. and Z.A.A.A.; validation: S.N.M.; investigation: M.A.A.-B. and Z.A.A.A.; resources: M.A.A.-B., Z.A.A.A. and S.N.M.; writing–original draft: M.A.A.-B., Z.A.A.A., and S.N.M.; visualization: Z.A.A.A. and S.N.M. All authors have read and agreed to the published version of the manuscript.

Conflict of interest: The authors state no conflict of interest.

Data availability statement: The datasets generated during and/or analysed during the current study are available from the corresponding author on reasonable request.

References

[1] Li F, Fan Y, Zhang X, Wang C, Hu F, Jia W, et al. Multi-feature fusion method based on EEG signal and its application in stroke classification. J Med Syst. 2020;44(2):39. doi: 10.1007/s10916-019-1517-9.

[2] Khairunizam W, Yean CW, Murugappan M, Junoh AK, Razlan ZM, Shahriman A, et al. An experimental framework for assessing emotions of stroke patients using electroencephalogram (EEG). In: Journal of Physics: Conference Series. vol. 1529. IOP Publishing; 2020. p. 052072. doi: 10.1088/1742-6596/1529/5/052072.

[3] Carino-Escobar RI, Carrillo-Mora P, Valdés-Cristerna R, Rodriguez-Barragan MA, Hernandez-Arenas C, Quinzannnos-Fresnedo J, et al. Longitudinal analysis of stroke patients brain rhythms during an intervention with a brain-computer interface. Neural Plasticity. 2019;2019(1):7084618. doi: 10.1155/2019/7084618.

[4] Grefkes C, Fink GR. Connectivity-based approaches in stroke and recovery of function. Lancet Neurol. 2014;13(2):206–16.

[5] Hachinski V, Donnan GA, Gorelick PB, Hacke W, Cramer SC, Kaste M, et al. Stroke: working toward a prioritized world agenda. Stroke. 2010;41(6):1084–99. doi: 10.1161/STROKEAHA.110.586156.

[6] Gao W, Cui Z, Yu Y, Mao J, Xu J, Ji L, et al. Application of a brain-computer interface system with visual and motor feedback in limb and brain functional rehabilitation after stroke: case report. Brain Sci. 2022;12(8):1083. doi: 10.3390/brainsci12081083.

[7] Al-Qazzaz NK, Alyasseri ZAA, Abdulkareem KH, Ali NS, Al-Mhiqani MN, Guger C. EEG feature fusion for motor imagery: A new robust framework towards stroke patients rehabilitation. Comput Biol Med. 2021;137:104799. doi: 10.1016/j.compbiomed.2021.104799.

[8] Al-Qazzaz NK, Ali SHB, Ahmad SA, Chellappan K, Islam M, Escudero J, et al. Role of EEG as biomarker in the early detection and classification of dementia. Scientif World J. 2014;2014(1):906038. doi: 10.1155/2014/906038.

[9] Jin J, Qu T, Xu R, Wang X, Cichocki A. Motor imagery EEG classification based on Riemannian sparse optimization and Dempster-Shafer fusion of multi-time–frequency patterns. IEEE Trans Neural Syst Rehabil Eng. 2022;31:58–67. doi: 10.1109/TNSRE.2022.3217573.

[10] Alyasseri ZAA, Khader AT, Al-Betar MA, Papa JP, Alomari OA, Makhadme SN. An efficient optimization technique of eeg decomposition for user authentication system. In: 2018 2nd International Conference on Biosignal Analysis, Processing and Systems (ICBAPS). IEEE; 2018. p. 1–6. doi: 10.1109/ICBAPS.2018.8527404.

[11] Al-Qazzaz NK, Sabir MK, Al-Timemy AH, Grammer K. An integrated entropy-spatial framework for automatic gender recognition enhancement of emotion-based EEGs. Med Biol Eng Comput. 2022;60(2):531–50. doi: 10.1007/s11517-021-02452-5.
[12] Al-Qazzaz NK, Hamid Bin Mohd Ali S, Ahmad SA, Islam MS, Escudero J. Automatic artifact removal in EEG of normal and demented individuals using ICA-WT during working memory tasks. Sensors. 2017;17(6):1326. doi: 10.3390/s17061326.
[13] Zhang Y, Nam CS, Zhou G, Jin J, Wang X, Cichocki A. Temporally constrained sparse group spatial patterns for motor imagery BCI. IEEE Trans Cybernetics. 2018;49(9):3322–32. doi: 10.1109/TCYB.2018.2841847.
[14] Chaudhary S, Taran S, Bajaj V, Siuly S. A flexible analytic wavelet transform based approach for motor-imagery tasks classification in BCI applications. Comput Methods Programs Biomed. 2020;187:105325. doi: 10.1016/j.cmpb.2020.105325.
[15] Alyasseri ZAA, Khadeer AT, Al-Betar MA, Abasi A, Makhadmeh S, Ali NS. The effects of EEG feature extraction using multi-wavelet decomposition for mental tasks classification. In: Proceedings of the International Conference on Information and Communication Technology; 2019. p. 139–46. doi: 10.1145/3321289.3321327.
[16] Tan P, Wang X, Wang Y. Dimensionality reduction in evolutionary algorithms-based feature selection for motor imagery brain-computer interface. Swarm Evolut Comput. 2020;52:100597. doi: 10.1016/j.swevo.2019.100597.
[17] Al-Qazzaz NK, Ali SHBM, Ahmad SA, Escudero J. Optimal EEG channel selection for vascular dementia identification using improved binary gravitation search algorithm. In: International Conference for Innovation in Biomedical Engineering and Life Sciences. Springer; 2017. p. 125–30. doi: 10.1007/978-981-10-7554-4_21.
[18] Al-Qazzaz NK, Ali SHM, Ahmad SA. Differential evolution based channel selection algorithm on EEG signal for early detection of vascular dementia among stroke survivors. In: 2018 IEEE-EMBS Conference on Biomedical Engineering and Sciences (IECBES). IEEE; 2018. p. 239–44. doi: 10.1109/IECBES.2018.8626684.
[19] Abasi AK, Khader AT, Al-Betar MA, Naim S, Makhadmeh SN, Alyasseri ZAA. A text feature selection technique based on binary multi-verse optimizer for text clustering. In: 2019 IEEE Jordan International Joint Conference on Electrical Engineering and Information Technology (JEEIT). IEEE; 2019. p. 1–6. doi: 10.1109/JEEIT.2019.8717491.
[20] Al-Qazzaz NK, Sabir MK, Ali SHBM, Ahmad SA, Grammer K. Multichannel optimization with hybrid spectral-entropy markers for gender identification enhancement of emotional-based EEGs. IEEE Access. 2021;9:107059–78. doi: 10.1109/ACCESS.2021.3096430.
[21] Faramarzi A, Heidarinejad M, Stephens B, Mirjalili S. Equilibrium optimizer: A novel optimization algorithm. Knowledge-Based Syst. 2020;191:105190. doi: 10.1016/j.knosys.2019.105190.
[22] Guo Z. Review of indoor emission source models. Part 1. Overview. Environ Pollut. 2002;120(3):533–49. doi: 10.1016/S0269-7491(02)00187-2.
[23] Al-Qazzaz NK, Ali SHM, Islam S, Ahmad S, Escudero J. EEG wavelet spectral analysis during a working memory tasks in stroke-related mild cognitive impairment patients. In: International Conference for Innovation in Biomedical Engineering and Life Sciences. Springer; 2015. p. 82–5. doi: 10.1007/978-981-10-0266-3_17.
[24] Hyvarinen A. Fast and robust fixed-point algorithms for independent component analysis. IEEE Trans Neural Netw. 1999;10(3):626–34. doi: 10.1109/72.761722.
[25] Escudero J, Hornero R, Abásolo D, Fernández A. Blind source separation to enhance spectral and non-linear features of magnetoencephalogram recordings. Application to Alzheimer's disease. Med Eng Phys. 2009;31(7):872–9. doi: 10.1016/j.medengphy.2009.04.003.
[26] James CJ, Hesse CW. Independent component analysis for biomedical signals. Physiol Measurement. 2005;26(1):R15. doi: 10.1088/0967-3334/26/1/r02.
[27] Al-Qazzaz NK, Hamid Bin Mohd Ali S, Ahmad SA, Islam MS, Escudero J. Selection of mother wavelet functions for multi-channel EEG signal analysis during a working memory task. Sensors. 2015;15(11):29015–35. doi: 10.3390/s151129015.
[28] Escudero J, Hornero R, Abásolo D, Fernández A. Quantitative evaluation of artifact removal in real magnetoencephalogram signals with blind source separation. Ann Biomed Eng. 2011;39(8):2274–86. doi: 10.1007/s10439-011-0312-7.
[29] Barbati G, Porcaro C, Zappasodi F, Rossini PM, Tecchio F. Optimization of an independent component analysis approach for artifact identification and removal in magnetoencephalographic signals. Clin Neurophysiol. 2004;115(5):1220–32. doi: 10.1016/j.clinph.2003.12.015.
[30] Mammone N, La Foresta F, Morabito FC. Automatic artifact rejection from multichannel scalp EEG by wavelet ICA. IEEE Sensors J. 2011;12(3):533–42. doi: 10.1109/JSEN.2011.2115236.
[31] Al-Qazzaz NK, Ali SHBM, Ahmad SA Islam MS Escudero J. Discrimination of stroke-related mild cognitive impairment and vascular dementia using EEG signal analysis. Med Biol Eng Comput. 2018;56:137–57. doi: 10.1007/s11517-017-1734-7.
[32] Al-Qazzaz N, Hamid Bin Mohd Ali S, Ahmad S, Islam M, Escudero J. Automatic artifact removal in EEG of normal and demented individuals using ICA–WT during working memory tasks. Sensors. 2017;17(6):1326. doi: 10.3390/s17061326.
[33] Braik M, Hammouri A, Atwan J, Al-Betar MA, Awadallah MA. White Shark Optimizer: A novel bio-inspired meta-heuristic algorithm for global optimization problems. Knowledge-Based Syst. 2022;243:108457. doi: 10.1016/j.knosys.2022.108457.
[34] Mirjalili S, Mirjalili SM, Lewis A. Grey wolf optimizer. Adv Eng Software. 2014;69:46–61. doi: 10.1016/j.advengsoft.2013.12.007.
[35] Mirjalili S, Gandomi AH, Mirjalili SZ, Saremi S, Faris H, Mirjalili SM. Salp Swarm Algorithm: A bio-inspired optimizer for engineering design problems. Adv Eng Software. 2017;114:163–91. doi: 10.1016/j.advengsoft.2017.07.002.
[36] Abualigah L, Diabat A, Mirjalili S, Abd Elaziz M, Gandomi AH. The arithmetic optimization algorithm. Comput Methods Appl Mech Eng. 2021;376:113609. doi: 10.1016/j.cma.2020.113609.